Contrib Mineral Petrol (1999) 135: 315–331

Elizabeth Cottrell · James E. Gardner
Malcolm J. Rutherford

Petrologic and experimental evidence for the movement and heating of the pre-eruptive Minoan rhyodacite (Santorini, Greece)

Received: 30 September 1997 / Accepted: 5 October 1998

Abstract Hydrothermal experiments combined with petrologic observations form the basis for a new two-stage model for the evolution of the pre-eruption Minoan magma chamber at Santorini, Greece. Ninety-nine percent of the erupted volume is two-pyroxene, rhyodacitic magma that had been stored at a temperature of ~885 °C, based on magnetite-ilmenite and QUILF geothermometry. The rest of the volume is basaltic to andesitic magma, which occurs as < 10 cm scoria clasts and as small inclusions in rhyodacite pumices. Petrologic observations show that these magmas mixed at different scales and at different times (i.e., multiple batches of mafic magma). Hydrothermal experiments were carried out on samples of rhyodacite and a mafic scoria in order to determine magma storage conditions and the mixing history of the two magmas. At 885 °C, the rhyodacite must have been stored at water-saturated pressures of ~50 MPa, based on its phase assemblage, matrix-glass composition, and crystal content. However, glass inclusions inside rhyodacitic plagioclase phenocrysts contain more than 6 wt% H_2O, indicating they formed at pressures > 200 MPa. In addition, the composition of the plagioclase hosts ($An_{56\pm6}$) of the inclusions require temperatures of 825 ± 25 °C at pressures > 200 MPa. This demonstrates that the Minoan rhyodacitic magma underwent a two-stage evolution, first crystallizing at ~ 825 °C and > 200 MPa, and then rinsing to a shallow ~50 MPa storage region with a concomitant rise in temperature to ~885 °C. We suggest that the episodic intrusion of mafic magmas provided the necessary heat and perhaps contributed to the ascent of the magma to shallow crustal depths where it re-equilibrated before the cataclysmic eruption. Phase equilibria suggest that much of the heating of the rhyodacite occurred in the shallow storage region. Thermal budget calculations suggest that the rhyodacite magma could have been heated by intrusions of basalt rising at reasonable upwelling rates and injected into the storage zone over several hundred years. Preservation of amphibole in the mafic scoria indicate that injection of mafic magma continued up until days before the cataclysmic eruption, perhaps triggering the event.

E. Cottrell[1] · J.E. Gardner[2] · M.J. Rutherford
Department of Geological Sciences, Brown University,
Providence, R.I. 02912, U.S.A.
Liz@ldeo.columbia.edu

Present address:
[1] Lamont-Doherty Earth Observatory,
Route 9W, Palisades, NY 10964
[2] Geophysical Institute, University of Alaska,
903 Koyukuk Drive, Fairbanks, AK 99775-7320, USA

Editorial responsibility: T.L. Grove

Introduction

The Bronze Age Minoan eruption at Santorini, Greece, began, after small phreatic explosions, with a plinian fall phase, followed by eruption of surges and cool, poorly fluidized pyroclastic flows, and ended with emplacement of hot pyroclastic flows (Bond and Sparks 1976; Heiken and McCoy 1984; Druitt et al. 1989; Sparks and Wilson 1990). A caldera about 65 km^2 in area formed as a result of the eruption (Heiken and McCoy 1984; Sparks and Wilson 1990; Druitt and Francaviglia 1992). About 99% of the magma erupted is compositionally uniform rhyodacite, with some mafic scoria erupted contemporaneously (Druitt et al. 1989). The mafic scoria is basaltic to andesitic in composition and occurs in a range of textures from 10-cm cauliform scoria to millimeter-sized blebs inside rhyodacite pumices. Overall, the scoria makes up ~1% of the Minoan deposit; its relative abundance increases in the fall deposit to about 20% at the top of the layer but tapers off in the overlying deposits. Rare crystal-rich pumices are also found in the deposit and are most likely partially melted granitoids from the walls of the magma chamber (Druitt et al. in press).

A complex pre-eruptive history for the Minoan rhyodacite was hinted at by Sigurdsson et al. (1990) and Gardner et al. (1996), who reported that glass inclusions in phenocrysts contained a significant amount of water,

many over 6 wt%. Given those high water contents, previous experimental works suggest that magmas similar in composition to the Minoan rhyodacite should crystallize amphibole (e.g., Rutherford et al. 1985; Gardner et al. 1995). Amphibole is absent, however, in the Minoan rhyodacite. We have investigated this apparent paradox of high water contents without phenocrystic amphibole. If amphibole existed at one time, its absence suggests that a major change occurred in the pre-eruption magma.

This study focuses on the evolution of the magma storage system for the rhyodacitic magma. We first briefly review petrologic investigations of the Minoan magmas and supplement those results with new data on both the rhyodacite and mafic scoria. To understand better the pre-eruptive histories of those two magmas, hydrothermal experiments were performed and the products are compared to natural samples. We find that the rhyodacite most likely underwent a heating event and polybaric migration within the crust, probably as a result of intrusion of mafic magma; physical and thermal models are proposed to explain this complex evolution.

Samples and techniques

Our samples consist of pumice and scoria clasts collected from the plinian fall layer of the Minoan deposit, at a site exposed in Thira quarry (Bond and Sparks 1976). Several homogeneous rhyodacitic pumices were hand crushed, sieved, and hand-picked for glass and mineral separates. Sample MIN93-10 consists of pumices from the base of the fall deposit, whereas MIN93-12 are pumices from the top. Thin sections were made of two mafic scoria clasts (CS-2 and CS-13) and three heterogeneous rhyodacitic pumices (SJG-100, SJG-200, and MINBAND) that contain small inclusions of mafic scoria.

Experimental methods

Two to five grams of rhyodacitic pumice (S-814; Table 1) and an andesitic scoria (CS-2; Table 1) were ground to a fine powder for use as starting material in most hydrothermal experiments; a few experiments used uncrushed pieces of CS-2. In all experiments, $Ag_{70}Pd_{30}$ tubes (2 or 5 mm in diameter) were used. These tubes were first welded at one end and then a weighted amount of distilled water and 30 to 200 mg of powder were added. The amount of distilled water added was sufficient to ensure that each experiment was run at water-saturated conditions, so that fluid pressure equaled total pressure. Experimental design then varied depending on the type of pressure vessel used. For runs in René cold-seal pressure vessels, the open end of the tube was welded shut. For runs in Titanium, Zirconium, Molybdenum, (TZM) pressure vessels, the sample tube was crimped shut and placed inside a larger (5 mm diameter) Ag tube welded at one end. A separate 3-mm Pt tube, with one end welded and containing weighted amounts of distilled water, Ni metal, and NiO powder, was then added to the large tube in order to monitor oxygen fugacity. The Pt tube was prevented from touching the tube containing the experimental powder by a piece of $Ag_{70}Pd_{30}$ metal. After the Pt tube was added, the large Ag tube was welded shut.

In many experiments, two charges were run to approach crystal-melt-vapor equilibrium from two directions. The powders used in these reversal experiments were aliquots of products of previously run experiments, chosen so that one charge was a "melting" experiment, using relatively crystal-rich material, and one charge was a "crystallization" experiment, using relatively melt-rich material. For runs in René vessels, the two tubes were run side by side in one pressure vessel. For runs in TZM vessels, the two tubes were added to the large tube before the buffer tube was added.

Oxygen fugacity in all experiments were buffered near the Ni-NiO buffer curve. This was accomplished in the René vessels by using a Ni filler rod and water as the pressurizing medium. We have found that this design buffers the charges at an f_{O_2} of 0.5 to 1 log unit above the Ni-NiO buffer curve (Geschwind and Rutherford 1992; Gardner et al. 1995). Experiments run in TZM vessels were buffered near Ni-NiO by adding $\sim$ 1 bar of methane to the Ar pressurizing medium. At the end of each TZM experiment, the contents of the Pt tube were inspected to assure that both Ni metal and NiO were present.

Analytical techniques

Matrix glass, glass inclusions, and minerals in the natural samples and matrix glass in the experimental products were analyzed using

Table 1 Minoan pumices: bulk and matrix glass compositions

Sample	S-814[a]	CS-2[a]	MIN93-10[b]	MIN93-12[b]	SJG-200[b]	SJG-100[b] (int.)	SJG-100[b] (quenched)	S-816-2[b]	S-816-2[b]
SiO_2[c]	69.07 (70)	56.33 (46)	73.57 (54)	73.91 (40)	72.18 (21)	73.09 (62)	72.75 (47)	73.42	71.98
TiO_2	0.45 (7)	0.88 (5)	0.29 (6)	0.28 (6)	0.37 (4)	0.26 (2)	0.32 (5)	0.29	0.44
Al_2O_3	15.08 (42)	17.15 (16)	13.86 (33)	13.71 (23)	14.44 (21)	13.90 (33)	13.96 (19)	13.77	14.48
FeO*	3.30 (10)	7.68 (5)	2.12 (17)	1.98 (10)	2.29 (9)	2.09 (8)	2.29 (19)	1.97	2.38
MnO	0.09 (7)	0.18 (7)	0.11 (4)	0.07 (4)	0.07 (4)	0.05 (3)	0.07 (5)	0.02	0.04
MgO	0.93 (2)	3.83 (1)	0.31 (6)	0.30 (3)	0.42 (4)	0.32 (3)	0.36 (6)	0.28	0.45
CaO	2.94 (5)	7.75 (19)	1.46 (13)	1.34 (11)	1.82 (13)	1.51 (13)	1.56 (16)	1.45	2.05
Na_2O	5.16 (25)	3.82 (7)	5.03 (18)	5.14 (15)	5.03 (24)	5.33 (48)	5.32 (22)	5.39	5.02
K_2O	2.81 (6)	1.25 (2)	3.25 (10)	3.27 (12)	3.37 (9)	3.45 (10)	3.38 (11)	3.42	3.15
n	3	3	12	10	13	5	10	1	1

[a] S-814 and CS-2 are bulk analyses of the rhyodacite pumice and mafic scoria clast, respectively, used for hydrothermal experiments. Both samples were crushed, fused to homogeneous glasses at 1300 °C and 1 bar for 5 h, and analyzed *n* number of times by electron microprobe

[b] Analyses of matrix glasses in rhyoldacite pumices. All samples are averages of *n* number of analyses, except data for S-816-2 which are representative analyses from that pumice. MIN93-10 and MIN93-12 are averages of glass separates made from homogeneous rhyodacite pumices. SJG-100 (Int.) is glass in the interior of pumice SJG-100, whereas SJG-100 (quenched) is the composition of glass next to rapidly quenched inclusions of andesite in SJG-100. SJG-200 is the average glass composition of a pumice that contains numerous inclusions of andesitic crystal clots. See text for further descriptions of each texture

[c] Oxides in wt%, with all Fe reported as FeO. Values in parentheses are estimated standard deviations on averages in terms of least units cited, thus 73.57 (54) indicates a standard deviation of 0.54 wt%. All analyses are normalized to total to 100 wt%

the Cameca Camebax electron microprobe at Brown University. Glass analyses were obtained using a 15 kV accelerating voltage, 10 nA beam current, and a defocused beam (10 μm diameter), using the techniques described by Devine et al. (1995). Precision and accuracy were monitored by repeatedly analyzing KN-18, a well characterized comenditic obsidian. Concentrations of Cl and S dissolved in glass inclusions in plagioclase phenocrysts were obtained using a 15 kV accelerating voltage, 30 nA beam current, and a focused beam. Mineral analyses were obtained using a 15 kV accelerating voltage, 15 nA beam current, and a focused beam.

Concentrations of H_2O, F, and B dissolved in glass inclusions in plagioclase phenocrysts were analyzed by secondary ion mass spectrometry (SIMS), using the IMS-3f ion microprobe (Cameca, France) at CRPS, Nancy, France. Sample preparation and analytical techniques used were those described by Gardner et al. (1995). Five rhyolitic glasses with 0.16 to 6.23 wt% dissolved water contents (Devine et al. 1995) were used as standards to create a calibration curve to reduce ion intensity ratios to water contents. Analyses of water contents dissolved in other rhyolitic standards, characterized by Fourier transform infrared spectroscopy (FTIR) and manometry, indicate that our analyses have a relative precision of about 7%. In addition, there is close agreement between the water contents and volatile contents estimated from the "difference" method, which equals 100 minus the total of the electron microprobe analysis. Precision of F and B analyses are about 20% and 10%, respectively.

Petrology and mixing of the rhyodacite and andesitic magmas

Druitt et al. (1989; in press) have described in detail the rhyodacitic and mafic scoria products of the Minoan eruption. Here, we describe the main features of the end-member magmas and the textures and petrology of their mingled hybrids (Fig. 1.) Our findings are based on observations of 25 pumices collected from the plinian fall layer of the deposit, but there are no significant petrological or compositional differences between pumices from the fall and pyroclastic flow layers of the deposit, and hence the entire 30 to 39 km^3 of rhyodacite magma erupted is considered homogeneous (Druitt et al. 1989; Sigurdsson et al. 1990).

Rhyodacitic magma

The compositionally uniform rhyodacite consists of highly vesicular rhyolitic glass with 10 to 20 vol.% phenocrysts of plagioclase, clinopyroxene, orthopyroxene, magnetite, and ilmenite ± apatite (Druitt et al. 1989). Matrix glasses are rhyolitic (73.5 to 74 wt% SiO_2), homogeneous, and do not vary compositionally between the base and top levels of the fall layer (Table 1). Plagioclase phenocrysts are generally euhedral, complexly zoned, and contain abundant glass inclusions. Despite this zoning, their rims are uniform in composition at $An_{39\pm2}$ (average of 14 grains). Plagioclase around the glass inclusions range in composition from An_{49} to An_{63} and average $An_{56\pm6}$ (Table 2). Rarely, plagioclase cores as anorthitic as An_{83} are found (Carey 1982).

The dominant Fe-Mg phenocrysts in the rhyodacite are ortho- and clinopyroxene (Druitt et al. 1989). The orthopyroxene phenocrysts are relatively unzoned and homogeneous (Table 3) and contain abundant inclusions of glass and Fe-Ti oxides. Clinopyroxenes are also unzoned, but two populations are found (Table 3): one is relatively enriched in MgO ($Mg\# = Mg/Mg+Fe^{2+} = 78$) and Al_2O_3, the other in FeO ($Mg\# = 70$). The-MgO-rich clinopyroxenes are similar in composition to those in mafic scoria inclusions in the rhyodacitic pumices, suggesting they are xenocrysts to the rhyodacite (Table 3). No phenocrystic amphibole is present in the rhyodacite, but rare hornblende inclusions have been found inside orthopyroxene grains (Fig. 1a). These amphiboles are iron rich (14 to 16 wt%) and have 9.5 to 10.5 wt% Al_2O_3 (Table 3). Orthopyroxene hosts to the amphibole inclusions are compositionally the same as other phenocrysts and thus are not xenocrystic to the rhyodacite.

Magnetite and ilmenite phenocrysts are ubiquitous in rhyodacitic pumices. Eleven magnetite-ilmenite pairs that are in contact with each other and surrounded by rhyolitic glass were analyzed (Table 4). Both phases are compositionally homogeneous and unzoned and typically are more than 100 μm in diameter. Compositionally, every magnetite-ilmenite pair is in equilibrium, according to their Mg and Mn contents (Bacon and Hirschmann 1988). Their compositions are distinct from those found in mafic scoria and inclusions, indicating that the pairs are inherent to rhyodacite magma (Table 4). A few discrete magnetites found in rhyodacite pumices are inherited from the mafic scoria, as witnessed by their compositions, but these can be easily distinguished.

Based on the compositions of the magnetite-ilmenite pairs, we estimate that the temperature of the rhyodacitic magma 885 ± 7 °C at an f_{O_2} of $10^{-11.7\pm0.2}$, using the mineral formula calculation scheme of Stormer (1983) and the algorithm of Anderson and Lindsley (1988), a procedure found to be the most accurate in reproducing temperatures of experimental samples (Geschwind and Rutherford 1992; Gardner et al. 1995). The errors quoted are small because they are standard deviations on the averages of eleven pairs. The oxygen fugacity is 0.5 ± 0.2 log units above the Ni-NiO oxygen buffer at 885 °C. In addition, when the magnetite and ilmenite compositions are used in conjunction with the pyroxene compositions, we calculate a temperature and oxygen fugacity using the Quartz Ulvospinel Ilmenite Fayalite (QUILF) algorithm (Anderson et al. 1993) that matches that from magnetite-ilmenite equilibria when silica activity is set to 0.9. This silica activity appears reasonable because there is no phenocrystic quartz. We conclude that the Fe-Mg phenocrysts in the Minoan rhyodacite record a temperature of 885 °C.

Glass inclusions in both plagioclase and pyroxene phenocrysts are rhyolitic and overlap considerably in composition, although those in pyroxenes are, on average, slightly more mafic (Table 2). There are no systematic variations in their major- and trace-element compositions, but there is considerable spread in water contents in the plagioclase glass inclusions; they range between 3.5 and 6.6 wt%. A similar spread is found in

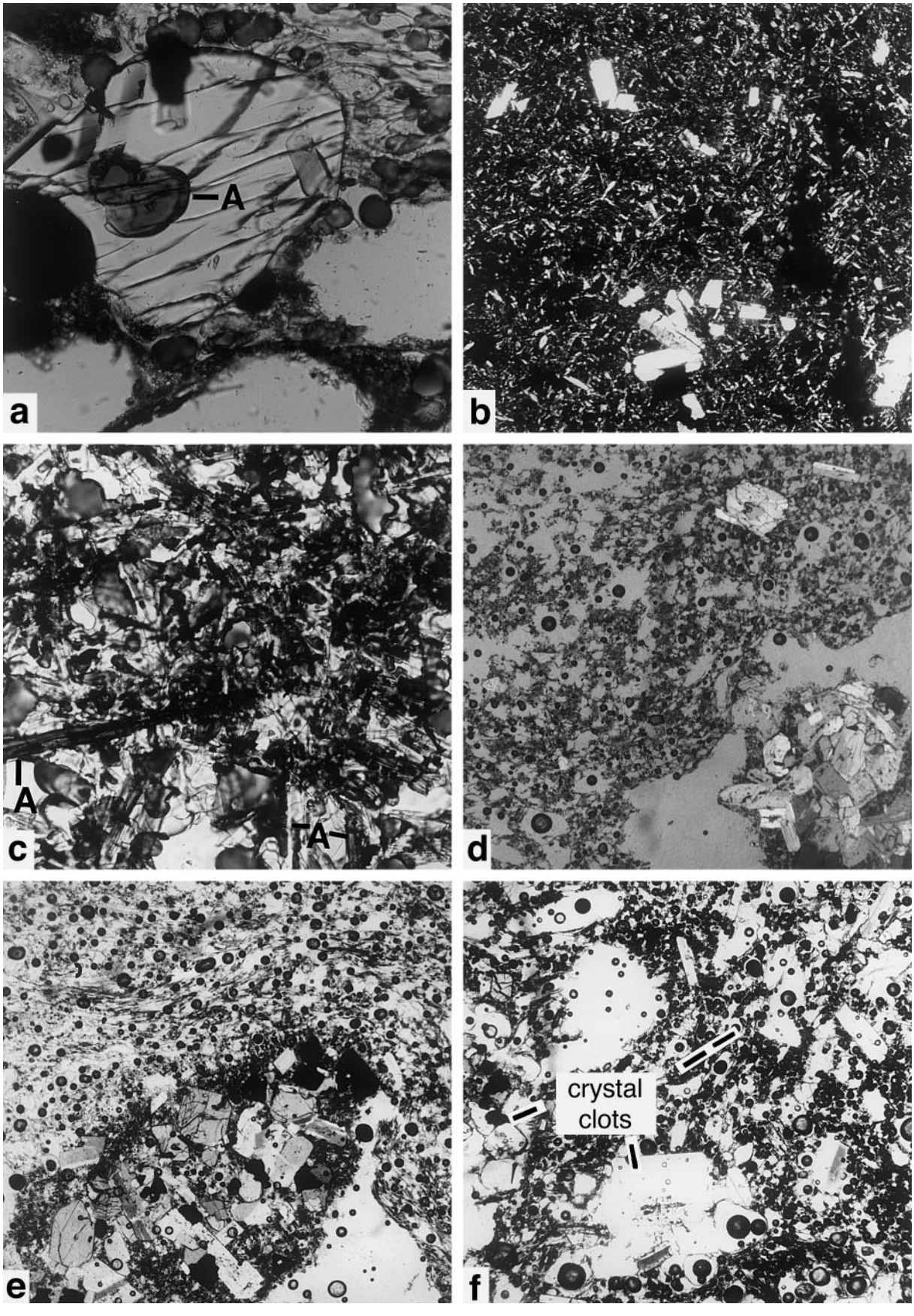
A
a
b
A
A
c
d
e
crystal
clots
f

◄

Fig. 1a Photomicrograph of relict amphibole inclusion (*A*) inside a rhyodacitic orthopyroxene phenocryst. The amphibole is about 70 μm in diameter. **b** Photomicrograph of mafic scoria clast (CS-2) showing relatively few phenocrysts in a highly crystallized groundmass rich in amphibole (see Fig. 1c). Width of field is 6 mm. **c** Photomicrograph of amphibole-rich groundmass of andesitic scoria (CS-2). Amphibole microlites (*A*) are 5 to 10 μm wide. **d** Photomicrograph of a 2-mm-wide inclusion of andesite in a rhyodacite pumice (MINBAND). The groundmass of this inclusion is rich in amphibole, similar to that of the mafic scoria (see Fig. 1c). **e** Photomicrograph of rapidly quenched inclusion of andesite in a rhyodacite pumice (SJG-100). The groundmass is a dark mass of microlites and vesicular glass. Width of field is approximately 4 mm. **f** Photomicrograph of rhyodacite pumice (SJG-200) containing small clots of crystals formed in the andesitic magma. Width of field is approximately 6 mm

the pyroxene glass inclusions (as measured by the difference between analytical total and 100%). These large spreads are most likely the result of partial degassing, as no other element varies nearly as extensively; for example, the entire range of K_2O contents is 0.31 wt%. The highest water contents average 6.2 (±0.3) wt% and are assumed to represent the original water content of the inclusions. The plagioclase glass inclusions also contain 3065 (±182) ppm Cl, 48 (±26) ppm S, and 732 (±123) ppm F, none of which vary with water content, indicating they did not degas as extensively.

Mafic scoria magma

About 1 to 2 vol.% of the Minoan deposit consists of scoria clasts that range in composition from basalt to andesite (Druitt et al. 1989). These scoria have been studied in detail (Druitt et al. 1989; in press), and so we mainly summarize those works, but we did study and analyze the phases in a few scoria clasts. The scoria contain 22 to 40 vol.% phenocrysts of plagioclase, clinopyroxene, orthopyroxene, olivine, and opaques (Fig. 1b). Although some of these phases are true phenocrysts to the scoria, many are clearly xenocrystic (Druitt et al. in press). We have found plagioclase phenocrysts containing glass inclusions that are colorless and have the same composition as those in the main rhyodacite; the "mafic" plagioclases contain brown, andesitic to dacitic glass inclusions. Considering the range in bulk composition and the common occurrence of xenocrysts, it is likely that most of the mafic magma was originally basalt to basaltic andesite. Below, we refer to the whole suite as mafic scoria and mafic magma.

The groundmass of the mafic scoria consists of small (< 100 μm) elongate crystals of plagioclase, clinopyroxene, orthopyroxene, magnetite, and vesicular silicate melt ± hornblende (Fig. 1c). Most of the clasts have groundmass hornblende, but usually in minor abundance and sporadically distributed (Druitt, pers. comm. 1996). In a few cases, however, it makes up 30 to 40% of the assemblage and is usually homogeneous in composition (Table 3). A few crystals deviate from true hornblende compositions and appear to be part hornblende and part pyroxene. These pyroxene-hornblende intergrowths may represent either hornblende growth in a clinopyroxene-bearing groundmass or partial decomposition of hornblende; the former is more likely because contacts between hornblende and groundmass vary widely in composition; TiO_2 varies from 5.2 to 11.6 wt%, Al_2O_3 from 2.6 to 5 wt%, and MgO from 1 to 2.5 wt% (Table 4). Magnetite phenocrysts are much more restricted in composition, but overlap those of the microlites.

Mixing textures between rhyodacitic and mafic magmas

We studied pumice clasts that have a variety of textures of mingling between the rhyodacitic and mafic magmas. More than half of the 25 pumices studied contain a small proportion of mafic material. This suggests that although the overall volume of mafic magma is small, interaction was extensive. Most of the mingled pumices are rhyodacites hosting small (< 3 mm) glomerocrysts (plagioclase + pyroxene + opaques) with or without a groundmass. The texture and composition of the glomerocrysts are similar to those in the mafic scoria clasts,

Table 2 Representative glass inclusions in plagioclase and pyroxene phenocrysts

Inclusion	Host[a]	SiO_2[b]	TiO_2	Al_2O_3	FeO*	MnO	MgO	CaO	Na_2O	K_2O	H_2O	Cl	S	F	B
8A	Plg (An_{56})	68.92	0.32	12.71	1.81	0.07	0.26	1.25	5.11	3.17	5.85	3079	100	842	24
9	Plg (An_{51})	70.07	0.27	12.81	1.79	0.09	0.28	1.26	5.20	3.13	3.98	3180	58	910	26
28A	Plg (An_{58})	70.76	0.31	13.00	1.77	0.04	0.27	1.32	4.95	3.03	4.87	2861	37	676	25
28B	Plg (An_{63})	69.66	0.34	13.13	2.04	0.13	0.30	1.38	5.31	3.12	5.05	3048	22	771	24
31C	Plg (An_{54})	69.00	0.30	12.96	1.84	0.08	0.31	1.41	4.79	3.13	6.20	3227	n.d.	685	23
30B	Plg (An_{49})	69.05	0.27	12.66	1.98	0.02	0.32	1.27	4.70	3.01	6.47	3030	48	738	16
26A	Plg (An_{59})	69.06	0.30	13.05	1.94	0.07	0.29	1.40	4.51	3.07	3.47	3081	34	870	25
13	Px	70.52	0.30	13.40	2.41	0.15	0.17	1.28	4.86	2.84	n.a.	n.a.	n.a.	n.a.	n.a.
15	Px	69.91	0.31	13.48	2.13	0.12	0.26	1.32	5.22	3.09	n.a.	n.a.	n.a.	n.a.	n.a.
19	Px	69.17	0.29	13.65	2.16	0.00	0.23	1.47	4.95	3.00	n.a.	n.a.	n.a.	n.a.	n.a.
27	Px	69.29	0.35	13.27	2.04	0.03	0.32	1.39	5.20	3.13	n.a.	n.a.	n.a.	n.a.	n.a.
28	Px	69.65	0.37	13.40	2.13	0.04	0.33	1.40	4.90	3.25	n.a.	n.a.	n.a.	n.a.	n.a.

[a] *Plg* plagioclase with average anorthite composition around the inclusion in parentheses, *Px* pyroxene (hosts not analyzed).
[b] Major elements (in wt%) and Cl and S (in ppm) by electron microprobe; H_2O (in wt%) and F and B (in ppm) by SIMS. Total Fe reported as FeO. *n.d.* not detected, *n.a.* not analysed.

Table 3 Compositions of pyroxenes and amphiboles in rhyodacite, mafic scoria, and mixtures

Sample[a]	MIN93-10	MIN93-10	MIN93-10	SJG-100	SJG-100	SJG-200	SJG-200	SJG-200	SJG-200
Type[a]	OPX	CPX (Fe-rich)	CPX (Mg-rich)	OPX	CPX	OPX (core)	OPX (rim)	CPX (core)	CPX (rim)
SiO_2[b]	51.71 (19)	51.33 (79)	50.78 (110)	53.39 (24)	51.59 (52)	52.52 (76)	51.82 (37)	51.96 (8)	51.83
TiO_2	0.19 (5)	0.39 (18)	0.67 (24)	0.26 (5)	0.46 (14)	0.26 (9)	0.27 (5)	0.27 (9)	0.23
Al_2O_3	0.55 (15)	1.35 (60)	2.82 (88)	1.41 (29)	2.25 (75)	1.66 (58)	1.42 (49)	1.12 (30)	0.90
FeO*	24.21 (69)	11.04 (21)	8.92 (19)	16.64 (31)	9.49 (30)	18.08 (63)	21.82 (106)	9.91 (75)	10.76
MnO	1.16 (10)	0.60 (7)	0.42 (6)	0.50 (5)	0.44 (6)	0.55 (10)	0.80 (17)	0.51 (12)	0.48
MgO	19.88 (36)	13.18 (23)	14.55 (65)	26.20 (20)	14.86 (21)	24.26 (63)	21.80 (65)	14.16 (49)	13.83
CaO	1.26 (6)	20.42 (24)	20.54 (30)	1.49 (8)	20.48 (38)	1.70 (24)	1.60 (30)	21.00 (4)	20.89
Na_2O	0.02 (2)	0.31 (5)	0.29 (6)	0.02 (1)	0.31 (1)	0.02 (1)	0.03 (2)	0.30 (1)	0.31
K_2O	0.01 (1)	0.01 (2)	0.01 (1)	0.01 (1)	0.00 (1)	0.01 (1)	0.01 (1)	0.00 (1)	0.01
Cr_2O_3	0.02 (3)	0.02 (2)	0.01 (2)	0.01 (1)	0.01 (1)	0.03 (3)	0.01(1)	0.04 (3)	0.00
Total	98.98	98.63	99.00	99.94	99.91	99.08	99.57	99.27	99.24
n	14	6	4	8	3	6	4	3	1

Sample[a]	CS-13	CS-2	S-816-2	S-816-2
Type[a]	A	A	A (Inclusion)	A (Microlites)
SiO_2[b]	41.20 (43)	40.77 (40)	43.18 (50)	43.96 (234)
TiO_2	2.26 (66)	3.12 (6)	2.88 (14)	2.10 (65)
Al_2O_3	12.21 (34)	12.40 (23)	9.86 (17)	11.29 (9)
FeO*	16.12 (54)	15.51 (10)	14.70 (40)	14.40 (92)
MnO	0.25 (4)	0.24 (4)	0.32 (9)	0.27 (5)
MgO	12.54 (25)	12.28 (3)	12.86 (8)	12.37 (75)
CaO	10.46 (42)	10.99 (11)	10.89 (14)	10.42 (55)
Na_2O	2.10 (12)	2.15 (15)	2.19 (9)	2.12 (12)
K_2O	0.36 (3)	0.39 (12)	0.46 (1)	0.48 (8)
Cr_2O_3	0.02 (2)	0.02 (2)	n.d.	n.d.
Total	97.52	97.89	97.35	97.41
n	7	5	1	4

[a] All data are averages of *n* number of analyses. MIN93-10 is a mineral separate from homogeneous rhyodacitic pumices. SJG-100 is a rhyodacitic pumice with rapidly quenched mafic scoria inclusions. SJG-200 is a rhyodacitic pumice with crystal-clot inclusions. CS-13 and CS-2 are cauliform mafic scoria. S-816-2 is a rhyodacitic pumice. *OPX* Ca-poor pyroxene, *CPX* Ca-rich pyroxene, *A* amphibole. See text for details

[b] Oxides in wt%, with all Fe reported as FeO. Values in parentheses are average standard deviations in terms of least units cited; thus 41.20 (43) indicates a standard deviation of 0.43 wt%. *n.d.* not determined

but their groundmass differs from inclusion to inclusion. In some cases, the groundmass is composed of microlites of abundant hornblende, plagioclase, pyroxenes, opaques, and vesicular glass, quite similar to that in the hornblende-bearing mafic scoria although the relative proportion of groundmass differs markedly (Fig. 1d). In other cases, the groundmass is a dark mass of microlites and abundant vesicular glass that appears to have quenched much faster than the hornblende-rich groundmass (Fig. 1e). We refer to these as ''rapidly quenched'' inclusions (Sample SJG-100). Finally, there are glomerocrysts that have no groundmass (Fig. 1f); these inclusions are referred to as ''crystal clots''.

Pyroxene phenocrysts in the rapidly quenched inclusions have a restricted range in composition (Fig. 2). Most pyroxenes in the crystal clots have compositions that overlap those in the rapidly quenched inclusions, but extend to more iron-rich (MgO poor) compositions. However, the rims of pyroxenes in the crystal clots that are in contact with the host glass differs significantly and almost equal those of the rhyodacite (Fig. 2).

Magnetite phenocrysts in the rapidly quenched inclusions have a restricted range in composition (Fig. 3). Magnetite phenocrysts in the crystal clots also have a restricted range in composition, regardless of location in the clots, yet their compositions match those of their host rhyodacite and not those in the rapidly quenched inclusions (Fig. 3).

The rhyodacite hosts of the andesite inclusions show some variability from normal rhyodacite pumices. The compositions of the matrix glasses, magnetites, and ilmenites vary with the different inclusion types (Tables 1, 4). The glass in samples that host the crystal clots (Sample SJG-200) is relatively uniform and, on average, more mafic than that in normal rhyodacite pumices (lower SiO_2, higher Al_2O_3, FeO*, MgO, CaO, and TiO_2). The glass that hosts the rapidly quenched inclusions (Sample SJG-100) is compositionally heterogeneous, with that near the inclusions being more mafic than that farther away. Fe-Ti oxides in the host of the crystal clots (SJG-200) differ slightly in composition from those of normal rhyodacite pumices (Fig. 3). Magnetite and ilmenite phenocrysts in the rhyodacite host of the rapidly quenched inclusions (Sample SJG-100) are compositionally identical to those of the normal rhyodacite pumices.

The textural and compositional relationships described above show that the rhyodacitic and mafic magmas mixed at different scales before or during

Table 4 Representative Fe-Ti oxides in rhyodacite and mafic scoria

Sample[a]	MIN93-10	MIN93-10	SJG-100	SJG-100	SJG-200	SJG-200
Type[b]	Mgt	Ilm	Mgt	Ilm	Mgt	Ilm
Phase[c]	(Rhyo; P)	(Rhyo; P)	(Rhyo; P)	(Rhyo; P)	(Rhyo; P)	(Rhyo; P)
TiO_2[d]	12.42 (49)	45.79 (45)	12.30 (27)	46.19 (13)	12.33 (29)	45.10
Al_2O_3	1.68 (7)	0.14 (3)	1.80 (4)	0.15 (2)	2.22 (4)	0.19
FeO*	80.81 (79)	49.76 (69)	78.88 (30)	48.22 (13)	77.13 (81)	47.11
MnO	0.66 (10)	0.97 (13)	0.65 (7)	0.95 (3)	0.54 (3)	0.75
MgO	1.81 (5)	2.16 (11)	1.22 (2)	0.95 (3)	1.65 (6)	2.83
Cr_2O_3	0.03 (3)	0.03 (4)	0.03 (1)	0.01 (1)	0.05 (5)	0.00
Total	97.41	98.85	94.88	97.76	93.93	96.00
n	22	27	4	2	9	
Sample	SJG-100	SJG-100	SJG-100	SJG-200	SJG-200	SJG-200
Type	(Incl; P)	(Incl; P)	(Incl; P)	(Incl; P)	(Incl; P)	(Incl; P)
Phase	Mgt	Mgt	Mgt	Mgt	Mgt	Mgt
TiO_2	8.90	8.95	9.14	12.47	12.65	12.64
Al_2O_3	4.23	4.27	4.32	2.28	2.28	2.26
FeO*	77.15	77.45	77.83	78.21	78.41	78.13
MnO	0.45	0.35	0.37	0.64	0.53	0.60
MgO	3.10	3.35	3.34	1.56	1.66	1.71
Cr_2O_3	0.04	0.03	0.06	0.08	0.06	0.05
Total	93.87	94.40	95.06	95.24	95.59	95.39
Sample	CS-13	CS-2	CS-2	CS-13	CS-13	CS-2
Type	(Scor; P)	(Scor; P)	(Scor; P)	(Scor; Gm)	(Scor; Gm)	(Scor; Gm)
Phase	Mgt	Mgt	Mgt	Mgt	Mgt	Mgt
TiO_2	7.98	7.11	8.33	9.64	7.21	10.30
Al_2O_3	4.55	2.93	4.47	3.28	3.88	3.72
FeO*	77.49	78.87	77.91	78.05	78.72	77.06
MnO	0.52	0.37	0.29	0.58	0.54	0.41
MgO	2.45	2.87	3.30	1.08	1.36	3.37
Cr_2O_3	0.11	0.15	0.06	0.03	0.00	0.04
Total	93.09	92.31	94.36	92.65	91.70	94.89

[a] Data are either averages of *n* number of analyses or individual analyses. MIN93-10 is a mineral separate from homogeneous rhyodacitic pumices. SJG-100 is a rhyodacitic pumice with rapidly quenched andesitic inclusions. SJG-200 is a rhyodacitic pumice with andesitic crystal clot inclusions. CS-13 and CS-2 are cauliform mafic scoria

[b] *Mgt* titanomagnetite, *Ilm* ilmenite

[c] *Rhyo* rhyodacite, *Incl* andesitic inclusion in rhyodacite, *Scor* mafic scoria clast, *P* phenocryst, *Gm* groundmass

[d] Oxides in wt%, with all Fe reported as FeO. Values in parentheses are average standard deviations in terms of least units cited; thus 12.42 (49) indicates a standard deviation of 0.49 wt%

eruption. In fact, this mixing was even more intimate because individual crystals from one magma are found in the other (see above). A few pyroxene and magnetite phenocrysts in the rhyodacite are from the mafic magma, and interestingly those xenocrysts lack diffusional profiles. A few plagioclase phenocrysts in the mafic scoria are from the rhyodacite. In addition, there are rare hornblende microlites in the matrix of one rhyodacite pumice that are compositionally the same as those in the mafic scoria groundmass (S-816-2; Table 3). The matrix glass of this pumice is bimodal (Table 1); some patches have a composition like normal rhyodacites and some have a composition like the host of the crystal clots (SJG-200).

In summary, the Minoan rhydoacitic magma last equilibrated at ~885 °C and contained a fairly homogeneous rhyolitic melt and phenocrysts of plagioclase, orthopyroxene, clinopyroxene, magnetite, and ilmenite. Glass inclusions contain up to ~6.2 wt% water and hornblende inclusions are present in some pyroxenes. A small volume of mafic magma was also erupted, and some samples of this magma crystallized abundant groundmass hornblende before erupting. Inclusions of mafic magma and crystals from it in the rhyodacite suggest that the two magmas mixed intimately. In the next section, we describe results from experiments performed to constrain the pre-eruptive conditions of the two magmas in order to elucidate better their pre-eruptive and mixing history.

Experimental results

Rhyodacite magma

All experiments on the rhyodacitic pumice (S-814; Table 2) were at pressures and temperatures above the solidus of the rhyodacite, so that melt is present in every experiment (Fig. 4). Titanomagnetite is present in all experiments, except at 975 °C and 200 MPa (Table 5). At slightly lower pressures and temperatures, clinopyroxene is the next liquidus phase, followed closely by orthopyroxene. The upper stability limit for plagioclase is at about 125 MPa at a temperature of

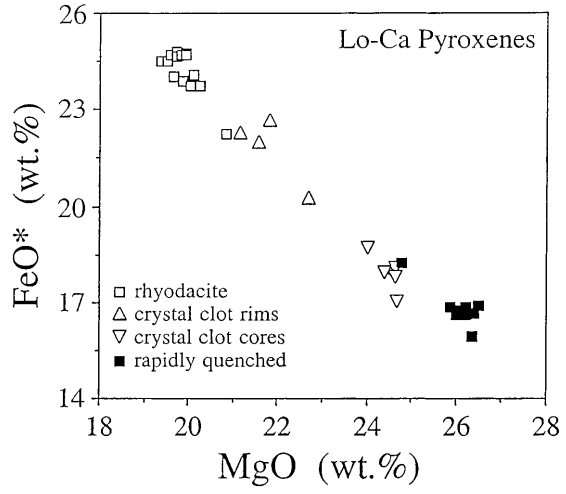

Fig. 2 Variation in Fe/Mg ratio in orthopyroxene phenocrysts from Minoan rhyodacite and andesite. *Open boxes* are core and rim analyses from the rhyodacite. *Filled boxes* are orthopyroxene phenocrysts in rapidly quenched mafic inclusions. *Inverted triangles* are orthopyroxene crystals inside crystal-clot inclusions; *triangles* are rims on those pyroxenes in contact with rhyodacite host (see text for descriptions)

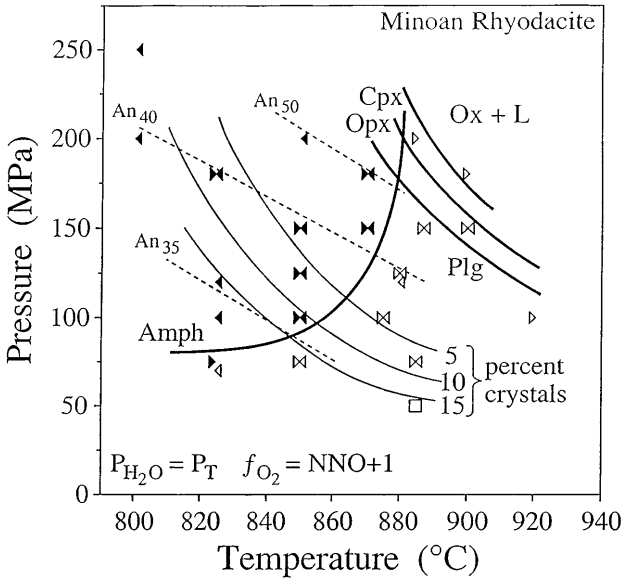

Fig. 4 Phase equilibria diagram for hydrothermal experiments on Minoan rhyodacite. All experiments were water saturated ($P_{H_2O} = P_{TOTAL}$). *Left-pointing triangles* represent crystallization experiments, *right-pointing triangles* represent melting. The experiment at 50 MPa and 885 °C is thought to be neither melting nor crystallization. *Filled symbols* are experiments in which amphibole grew. *Heavy curves* are stability boundaries for plagioclase, pyroxenes, and amphibole. Silicate melt and Fe-Ti oxides are present in every experiment. *Thin curves* are isopleths of equal crystal content in the experimental products based on the K_2O contents in their glasses. *Dotted lines* are isopleths of anorthite content of plagioclase

900 °C and above 180 MPa at 875 °C. Amphibole grew in many of our experiments, even though it is not a stable phase in the natural rhyodacitic pumice (Fig. 4). At 870 °C, amphibole is stable at pressures above about 125 MPa, whereas it is stable at pressures above 100 MPa at 850 °C. It is not stable at temperatures above 880 °C over the pressure range explored (Fig. 4). It could be argued that because we used a powdered sample for our starting material, we altered the starting conditions by, for example, exposing An-rich cores in plagioclase to the melt. We find, however, that the phase relationships, as well as the melt compositions (see next paragraph, below), are consistent between crystallization and melting experiments (Table 4). This indicates that phase equilibria for the rhyodacite were not measurably affected by the incorporation of phenocrystic cores.

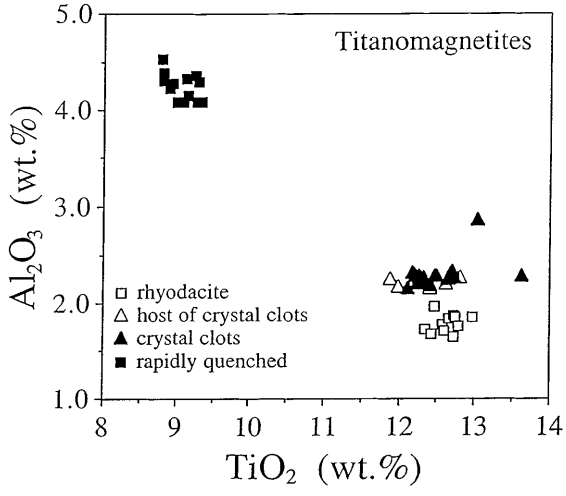

Fig. 3 Variation in Ti/Al ratio in magnetite phenocrysts from Minoan rhyodacite and andesite. *Open boxes* are phenocrysts from the rhyodacite. *Filled boxes* are phenocrysts in rapidly quenched mafic inclusions. *Filled triangles* are phenocrysts in crystal clot inclusions, whereas *open triangles* are phenocrysts in rhyodacite host of the crystal clot inclusions (see text for descriptions)

Melt (quenched to glass) is the most abundant phase in the experiments and its composition varied systematically with pressure and temperature (Table 6). In reversed experiments that ran sufficiently long, the melts are the same composition (Fig. 5). Lowering the water pressure at constant temperature causes concentrations of SiO_2 and K_2O to increase and concentrations of FeO, MgO, and CaO to decrease. These variations in residual melt composition also occur as temperature decreases at constant pressure (Fig. 6). In addition, the Mg# ($Mg/Mg + Fe_{total}$) of the glass decreases with lower temperature and lower pressure. At high pressures (~200 MPa), Al_2O_3 contents increase as temperature increases to 875 °C and then decrease as temperature increases further, reflecting the fact that plagioclase is unstable above this temperature.

Because K_2O is incompatible in all minerals crystallized in our experiments, we can use its abundance to estimate the amount of crystals present. Curves calculated to show 5, 10, and 15 wt% crystallinity are contoured in Fig. 4. These curves parallel the liquidus curves for plagioclase and pyroxene, indicating that

Table 5 Conditions of experiments on Minoan rhyodacite pumice

Run	Starting Material[a]	Temperature (°C)	Pressure (MPa)	Duration (h)	Products[b]
LS1	S-814	880	120	28	G, Plg, Pyx, Ox
LS2	S-814	825	120	66	G, Plg, Pyx, Ox, A
LS3	LS1	850	100	288	G, Plg, Pyx, Ox, A
LS4	LS2	850	100	288	G, Plg, Pyx, Ox, A
LS5A	LS1	850	75	240	G, Plg, Pyx, Ox
LS5B	LS2	850	75	240	G, Plg, Pyx, Ox
LS6	LS1	850	150	95	G, Plg, Pyx, Ox, A
LS7	LS2	850	150	95	G, Plg, Pyx, Ox, A
LS8	LS1	850	125	144	G, Plg, Pyx, Ox
LS9	LS2	850	125	144	G, Plg, Pyx, Ox, A
LS10	S-814	975	200	36	G
LS11	S-814	920	100	12	G, Plg, Pyx, Ox
LS12	S-814	825	100	20	G, Plg, Pyx, Ox, A
LS13	S-814	880	125	20	G, Plg, Pyx, Ox
LS14	LS11	880	125	20	G, Plg, Pyx, Ox
LS15	LS12	875	100	42	G, Plg, Pyx, Ox
LS16	LS11	875	100	42	G, Plg, Pyx, Ox
LS17	LS11	900	150	42	G, Plg, Pyx, Ox
LS18	LS12	900	150	42	G, Plg, Pyx, Ox
LS19	S-814	950	150	20	G, Plg, Pyx, Ox
LS22	S-814	825	180	88	G, Plg, Pyx, Ox, A
LS24	S-814	825	70	168	G, Plg, Pyx, Ox
LS25A	LS22	870	180	42	G, Plg, Pyx, Ox, A
LS25B	LS19	870	180	42	G, Plg, Pyx, Ox, A
LS26	S-814	900	180	44	G, Ox
LS27	LS19	887	150	44	G, Plg, Pyx, Ox
LS28	LS22	887	150	44	G, Plg, Pyx, Ox
LS29	S-814	870	150	16	G, Plg, Pyx, Ox, A
LS30	LS22	870	150	16	G, Plg, Pyx, Ox, A
LS31	S-814	885	200	44	G, Pyx, Ox
LS32	LS29	870	150	51	G, Plg, Pyx, Ox
LS33	LS30	870	150	51	G, Plg, Pyx, Ox, A
LS39	S-814	885	50	72	G, Plg, Pyx, Ox
G144A	LS26	800	200	120	G, Plg, Pyx, Ox, A
LS53A	LS31	885	75	24	G, Plg, Pyx, Ox
LS53B	S-814	885	75	72	G, Plg, Pyx, Ox
G163	LS26	850	200	145	G, Plg, Pyx, Ox, A
G164	LS26	800	250	188	G, Plg, Pyx, Ox, A
L7	LS24	825	75	264	G, Plg, Pyx, Ox

[a] Starting material was either powder of a crushed, natural rhyodacite pumice (S-814) or an aliquot of pre-run sample, designated by its run number

[b] Run products are *G* melt (quenched to glass), *Plg* Plagioclase, *Pyx* pyroxene, *Ox* magnetite ± ilmenite, and *A* amphibole

these phases, followed by hornblende, are the dominant crystallizing phases. Overall, the abundance of crystals increases with lower temperature and/or pressure in these water-saturated experiments.

Mafic scoria magma

Experiments were also run on a mafic scoria (CS-2; Table 1) at temperatures from 865 to 910 °C and over pressures between 50 and 150 MPa (Table 7). These experiments were all water saturated. The range of conditions investigated was limited because we were interested in the stability limit of groundmass amphibole in the andesite. Amphibole grew at water pressures above 60 MPa at 870 °C and above 75 MPa and at 885 °C (Fig. 7). At 150 MPa, amphibole is stable only at temperatures below 900 ± 10 °C. Silicate melt is present in all of these experiments, but its abundance decreases dramatically with lower temperature and pressure, until there is almost none left at 50 MPa and 870 °C.

Some phenocrysts in the mafic scoria are xenocrysts, and so using a crushed powder as a starting material may not be entirely appropriate. In order to check our results, a series of experiments were run using uncrushed chips of the mafic scoria such that most reactions involve only the groundmass phase (± phenocryst rims). This series shows that at 885 °C and 75 MPa amphibole remained stable up to 48 h, began to breakdown after 72 h, and was extensively reacted in 96 h (Table 7). This is consistent with our powder experiments that showed amphibole was not stable at 75 MPa and 885 °C.

Comparing amphibole stability in the rhyodacite and andesite experiments, we find that at a given temperature, higher pressures are required to grow amphibole in the rhyodacite than in the andesite. Similarly, at a given pressure amphibole is stable at higher temperatures in

Table 6 Glass compositions of rhyodacite experiments

Run[a]	SiO_2[b]	TiO_2	Al_2O_3	FeO	MnO	MgO	CaO	Na_2O	K_2O	Total	*n*
LS3	68.95	0.25	13.61	1.88	0.09	0.31	1.55	4.41	3.02	94.07	5
LS4	68.22	0.25	13.46	1.85	0.08	0.29	1.6	4.71	3.07	93.54	6
LS5B	70.63	0.27	13.15	1.61	0.06	0.23	1.29	4.79	3.38	95.42	6
LS7	67.29	0.32	14.05	2.07	0.08	0.37	2.04	4.78	2.79	93.79	8
LS8	66.72	0.32	14.35	2.27	0.07	0.38	1.95	4.83	2.98	93.86	7
LS9	66.83	0.31	14.13	2.38	0.07	0.46	2.09	4.9	2.83	93.99	7
LS11	71.72	0.35	13.83	2.64	0.05	0.42	1.73	4.77	3.22	98.74	5
LS13	66.24	0.34	14.14	2.34	0.04	0.49	2.11	4.84	2.75	93.3	7
LS14	66.56	0.34	14.42	2.31	0.06	0.54	2.15	4.92	2.79	94.09	6
LS15	66.24	0.31	13.77	2.17	0.08	0.48	2.11	4.7	2.77	92.64	6
LS16	67.25	0.35	14.07	2.11	0.09	0.48	1.97	4.75	2.84	93.91	8
LS18	70.4	0.41	14.09	2.41	0.05	0.46	1.86	4.99	2.99	97.68	6
LS22	66.34	0.23	13.74	1.74	0.04	0.25	1.77	4.46	2.92	91.49	4
LS25A	66.37	0.33	14.61	2.51	0.06	0.47	2.22	4.67	2.79	94.03	7
LS25B	65.58	0.39	14.05	2.51	0.08	0.53	2.26	4.23	2.75	92.38	6
LS26	66.42	0.42	14.02	2.67	0.06	0.71	2.43	4.65	2.64	94.02	5
LS31	65.37	0.36	14.12	2.63	0.09	0.63	2.44	4.53	2.68	92.85	6
LS33	65.8	0.36	14.52	2.66	0.06	0.6	2.47	4.63	2.72	93.82	8
LS39	69.81	0.32	13.15	2.12	0.06	0.29	1.39	4.6	3.26	95.00	6
G144A	68.66	0.19	13.42	1.14	0.10	0.21	1.53	4.43	3.08	92.76	6
LS53B	67.23	0.37	13.77	2.53	0.08	0.43	1.94	4.57	2.95	93.87	6
LS53A	67.76	0.33	13.98	2.43	0.07	0.49	2.05	4.70	2.84	94.65	6
G163	66.22	0.25	14.11	1.35	0.05	0.30	2.09	4.64	2.77	91.78	6
G164	66.81	0.16	14.04	1.22	0.08	0.19	1.87	4.54	2.84	91.75	6
L7	71.13	0.28	12.71	1.44	0.06	0.22	1.07	4.63	3.42	94.96	5

[a] See Table 5 for experimental run conditions
[b] Oxides in wt%, with all Fe reported as FeO. Values are averages of *n* number of analyses

the andesite relative to the rhyodacite. For example, at 150 MPa amphibole is stable in the andesite to temperatures at least 30 °C above where it is stable in the rhyodacite. In addition, the experiments performed on scoria rock chips show that the groundmass amphibole present in the mafic scoria must have grown at water pressures greater than 75 MPa, assuming a temperature equal to that of the rhyodacite (885 °C); if it was hotter, then higher water pressures would be necessary.

Discussion

Petrologic observations indicate that the rhyodacitic and mafic magmas erupted during the Minoan event mixed at different scales. In the following sections, we use these observations in conjunction with experimental results to infer the pre-eruptive, pressure-temperature conditions of the magmas and their mixing history. The experimental data are for water saturation, and so the rhyodacite is initially assumed to have been water saturated; this assumption is discussed and justified later in the discussion.

Final equilibration conditions of the rhyodacitic magma

Just before erupting, the rhyodacite magma consisted of rhyolitic melt and phenocrysts of plagioclase (rims of $An_{39\pm2}$), orthopyroxene, clinopyroxene, titanomagnetite, and ilmenite. We estimate from titanomagnetite-ilmenite and QUILF geothermometry that this magma last equilibrated at a temperature of 885 (± 7) °C with an f_{O_2} of about 0.5 log units above the Ni-NiO buffer curve. The most abundant phenocryst in the magma is plagioclase, and at 885 °C plagioclase is stable only below 180 MPa (Fig. 4). In addition, the overall crystallinity of the natural rhyodacite is between 10 and 20 vol.%, which at 885 °C further restricts pressure to below 75 MPa. Finally, amphibole is stable at temperatures less than 880 °C at 180 MPa, yet the rhyodacite does not contain stable amphibole. Together, these arguments indicate a final pre-eruption equilibration of the rhyodacite at a pressure below 75 MPa at a temperature of 885 °C.

The pressure at which the rhyodacite last equilibrated can be further constrained by comparing experimental glass compositions with the natural matrix glass (Fig. 5). At 885 °C, the melt composition in the experiments approximates that of the matrix glass at water pressures of about 50 MPa. This rhyolitic melt is in equilibrium with plagioclase, orthopyroxene, clinopyroxene, titanomagnetite, and ilmenite, the phenocryst phase assemblage of the natural rhyodacite. We conclude, therefore, that the rhyodacite last equilibrated at 885 °C and about 50 MPa (Fig. 8).

Conditions of the rhyodacitic magma recorded by glass inclusions

Because the Minoan magma last equilibrated at a water pressure of 50 MPa, the coexisting melt could contain at most 2.5 to 3.0 wt% H_2O, based on studies of water

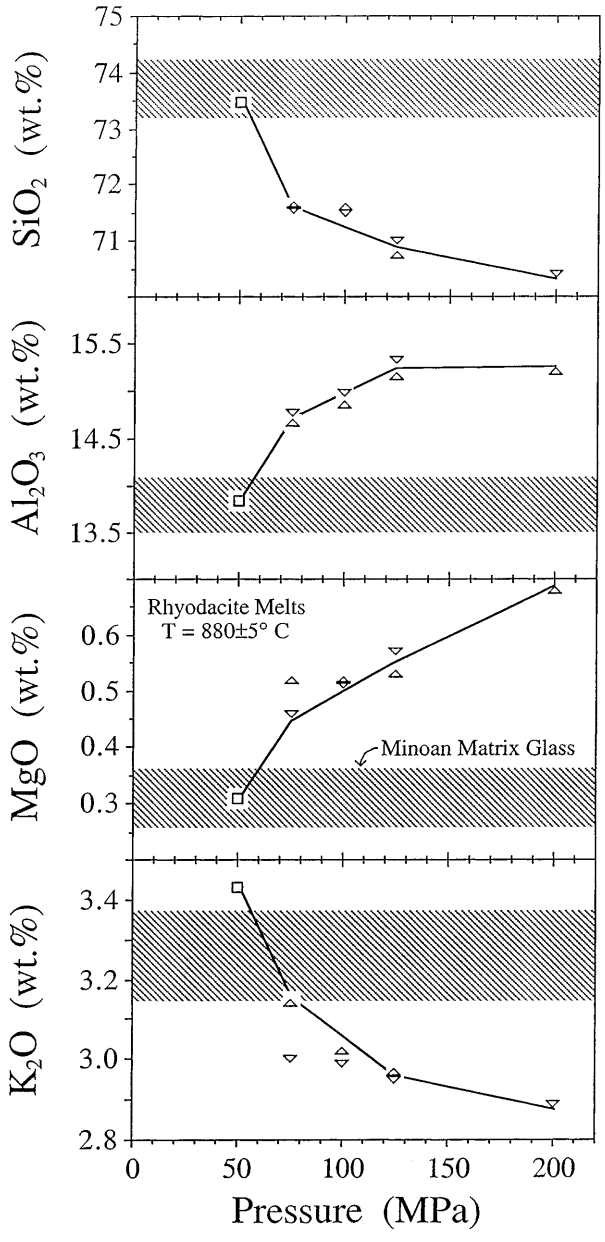

Fig. 5 Variation in experimental glass composition as a function of pressure at a temperature between 875 and 885 °C. *Arrows* point in direction that glass composition is changing based on whether it is a crystallization or melting experiment. *Lines* represent approximate variations based on the experiments at 880 and 885 °C, assuming that the crystallization experiment at 75 MPa better represents the glass composition at that pressure. *Shaded region* represents the average composition ($\pm 1\sigma$) of the matrix glass in the Minoan rhyodacite

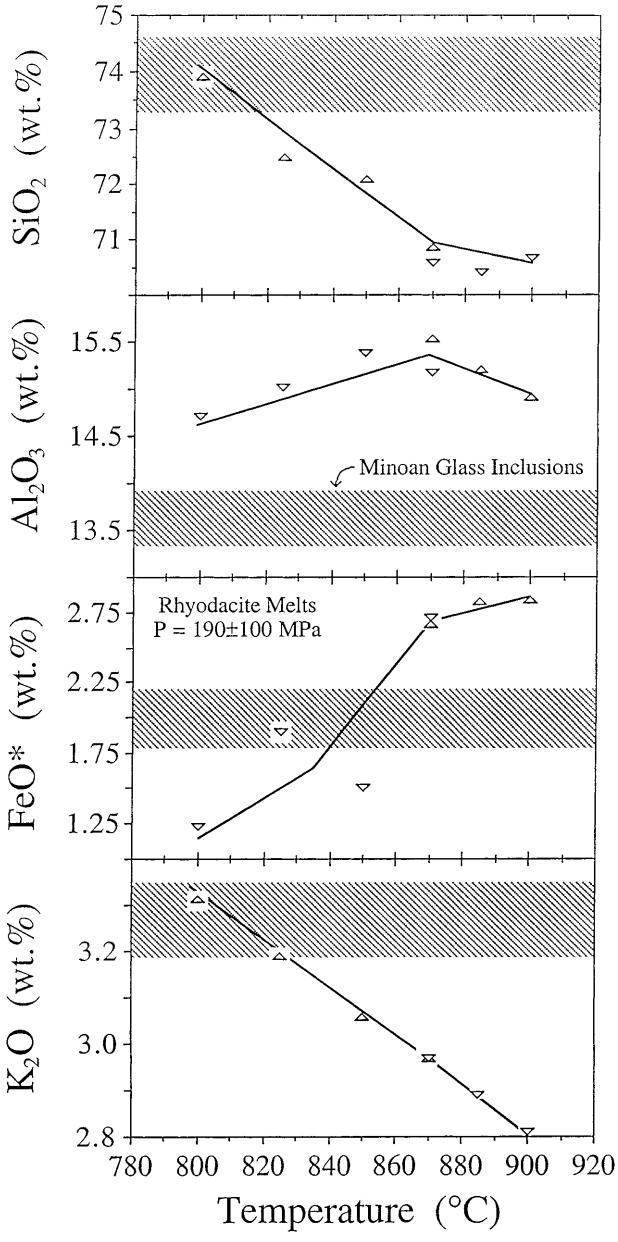

Fig. 6 Variation in experimental glass composition as a function of temperature at a pressures between 180 and 200 MPa. *Arrows* point in direction that glass composition is changing based on whether it is a crystallization or melting experiment. *Lines* represent approximate variations based on the experiments at 180 MPa, assuming that the crystallization experiment at 875 °C better represents the glass composition at that pressure. *Shaded region* represents the average composition ($\pm 1\sigma$) of the glass inclusions in plagioclase phenocrysts from the Minoan rhyodacite

solubility in rhyolitic melts (Silver et al. 1990; Fogel 1989; Blank et al. 1993). These water contents are significantly lower than the ~6.2 wt% water found dissolved in glass inclusions (Table 2). In fact, a water content of 6.2 wt% requires water pressures of 210 to 240 MPa. At such pressures, however, the glass inclusions could not have formed when the rhyodacite was 885 °C, because plagioclase is not stable in this bulk composition at those conditions (Fig. 4). The glass inclusions were therefore trapped at very different conditions from those at which the rhyodacitic magma last equilibrated.

The compositions of the glass inclusions are similar to the experimental glasses produced in the rhyodacite at pressures at 180 to 200 MPa and relatively low temperatures, although there is no exact match (Fig. 6). Such comparisons assume that the bulk composition from which the inclusions were trapped is the same as the final Minoan rhyodacite. As mentioned above, pet-

Table 7 Conditions of experiments on Minoan andesite scoria

Run	Starting material[a]	Temperature (°C)	Pressure (MPa)	Duration (h)	Products[b]
LS34	CS-2p	970	100	68	G, Plg
LS35	LS34	887	120	48	G, Plg, Pyx, Ox, A
LS38	LS34	885	75	48	G, Plg, Pyx, Ox
LS40	LS34	885	50	48	G, Plg, Pyx, Ox
LS42I	CS-2p	870	120	24	G, Plg, Pyx, Ox, A
LS42O	LS34	870	120	24	G, Plg, Pyx, Ox, A
LS44	CS-2p	1050	150	6	G, Plg
LS46	CS-2p	880	100	20	G, Plg, Pyx, Ox, A
LS47	CS-2p	865	100	24	G, Plg, Pyx, Ox, A
LS48	LS34	880	100	20	G, Plg, Pyx, Ox, A
LS49	LS47	885	120	24	G, Plg, Pyx, Ox, A
LS50L	CS-2p	890	150	43	G, Plg, Pyx, Ox, A
LS50S	LS44	890	150	43	G, Plg, Pyx, Ox, A
LS51L	CS-2p	910	150	43	G, Plg, Pyx, Ox
LS51S	LS44	910	150	43	G, Plg, Pyx, Ox
LS52A	CS-2p	870	75	31	G, Plg, Pyx, Ox, A
LS52B	LS38	870	75	31	G, Plg, Pyx, Ox
LS54	CS-2p	870	50	48	G, Plg, Pyx, Ox
LS55	LS51S	870	50	48	G, Plg, Pyx, Ox
G150	CS-2p	885	200	24	G, Plg, Pyx, Ox, A
G162	G150	885	50	49	G, Plg, Pyx, Ox, [A]
G165	CS-2p	885	50	48	G, Plg, Pyx, Ox
L4	CS-2c	885	75	24	G, Plg, Pyx, Ox, A
L5A	CS-2c	885	75	48	G, Plg, Pyx, Ox, A
L5B	L4	885	75	48	G, Plg, Pyx, Ox, [A][c]
L6	L5A	885	75	48	G, Plg, Pyx, Ox, [[A]][c]

[a] All experiments used material from a single mafic scoria clast (CS-2; Table 1) as crushed powder (CS-2p), chips of the scoria clast (CS-2c), or an aliquot of pre-run sample (designated by its run number).
[b] Run products are *G* melt (quenched to glass), *Plg* plagioclase, *Pyx*, pyroxene, *Ox*, magnetite ± ilmenite, *A* stable amphibole, [*A*] abundant amphibole showing reaction relations, and [[*A*]] little amphibole left
[c] Phase relationships in L5B and L6 indicate that amphibole is unstable at these conditions, but run times were too short to record significant reaction

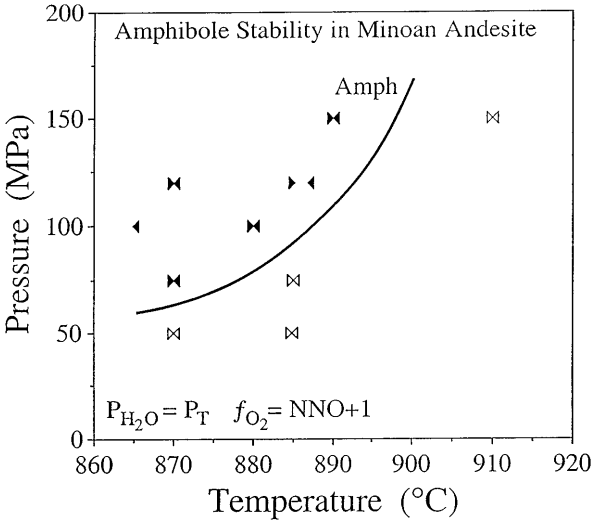

Fig. 7 Phase equilibria diagram for hydrothermal experiments on Minoan andesite. All experiments were run with excess water, so that total pressure equals water pressure. *Left-pointing triangles* represent crystallization experiments, *right-pointing triangles* represent melting. *Filled symbols* are experiments in which amphibole grew. *Heavy curve* is the stability boundary for amphibole. Plagioclase, pyroxene, FeTi oxides and silicate melt are present in all experiments

rologic observations suggest that there was intimate interaction between the rhyodacitic and mafic magmas, and so it is possible that the rhyodacite was previously more silicic in composition. Despite this uncertainty, however, we know that the glass inclusions were trapped at significantly higher pressures and lower temperatures than the final rhyodacite equilibration conditions of 50 MPa and 885 °C, based on the water contents in glass inclusions and the stability of plagioclase. Plagioclase is not stable above 870 °C at 200 MPa in the rhyodacite, and if the bulk composition was more silicic, this temperature would be lower. The glass inclusions are in contact with plagioclase of $An_{56\pm5}$; the experimental plagioclase composition at 850 °C and 200 MPa is An_{50}, supporting the idea of a low entrapment temperature. The low S contents in the inclusions (highest value measured is 112 ppm) are also consistent with them being trapped at low temperatures, based on sulfur solubility in silicate melts (Carroll and Rutherford 1985; Rutherford and Devine 1996).

We suggest that the glass inclusions formed when the magma was at 210 to 240 MPa and 825 ± 25 °C. At those conditions, our experiments imply that the magma would not only contain plagioclase and pyroxene but also amphibole (Fig. 4). This would almost certainly be true even if the bulk composition were more silicic than the final rhyodacite. Amphibole inclusions are found in pyroxene phenocrysts (Fig. 1a). Compositions of these inclusions match very closely those of amphiboles produced at 850 °C and 200 MPa. The presence of horn-

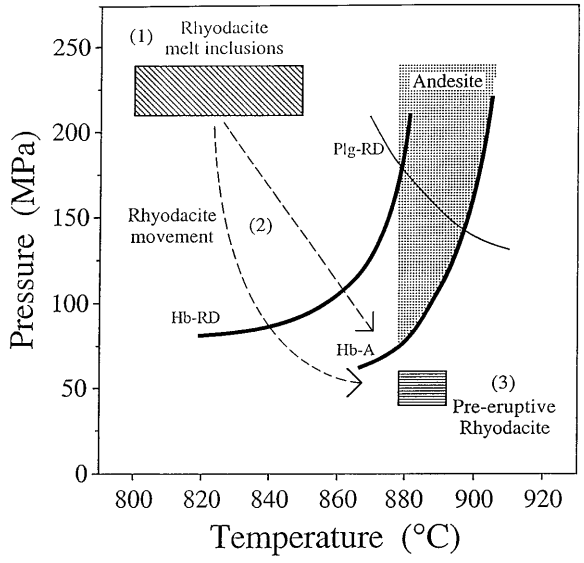

Fig. 8 Pressure-temperature conditions inferred for the Minoan magmas. *Heavy curves* are the upper stability limits of amphibole in the rhyodacite (Hb-RD) and andesite (Hb-A); *thin curve* shows the upper stability limit of plagioclase (Plg) in the rhyodacite. The *horizontally ruled box* marks conditions at which the Minoan rhyodacite last equilibrated, whereas the *diagonally ruled box* marks the likely conditions at which melt inclusions in plagioclase phenocrysts formed. The *P-T* path followed by magma in moving between the high and low pressure storage regions is unknown. Mafic scoria containing amphibole microlites must have passed through the *dotted region*

blendes inside pyroxenes appears to record, like the glass inclusions, a period when the magma was stored at higher pressures and lower temperatures than the final equilibration conditions.

Interaction between the rhyodacitic and mafic magmas

The data above suggest that the Minoan rhyodacitic magma was at one time stored at 210 to 240 MPa and 825 ± 25 °C, but then re-equilibrated at 50 MPa and 885 °C (Fig. 8). Magnetite and ilmenite phenocrysts that are ~100 μm diameter are homogeneous. This indicates that the time spent at 885 °C would have to be at least months in order to rehomogenize these phenocrysts to the higher temperature by diffusion (Nakamura 1995; Venezky and Rutherford, in press). This places a minimum on the amount of time required to heat the rhyodacite. In addition, much of the heating probably occurred at low pressures, because if it occurred at higher pressures, plagioclase would have totally melted (Fig. 4).

The most likely cause of the thermal and pressure change in the rhyodacite was intrusion of mafic magma into the storage system. A long history of injections is manifested by the various mixing textures of the rhyodacite and mafic scoria (Fig. 1). Some mafic scoria quenched rapidly in the rhyodacite. The matrix glass that hosts this rapidly quenched mafic scoria is heterogeneous, suggesting little time for homogenization (SJG-100; Table 1). In addition, some of the mafic scoria, which erupted along with the rhyodacite from the 50 MPa storage region, contain groundmass amphibole with no signs of breakdown. These amphiboles probably grew during cooling and ascent of the mafic magma to the shallow reservoir (Fig. 9). However, these scoria could have spent no more than a couple of days of 50 MPa, or hornblende would have broken down in a reaction with the groundmass melt. This suggests that some mafic magma was injected into the rhyodacite very shortly (hours to days?) before eruption. In support of this conclusion, we have found magnetite phenocrysts from the mafic magma in contact with rhyodacite groundmass and these magnetites lack any sign of diffusional exchange with the matrix. This implies a final mixing event less than a few days before eruption (Nakamura 1995; Venezky and Rutherford, in press).

The crystal clots from the mafic magma in the rhyodacite show evidence of an earlier emplacement; their pyroxenes indicate that there was enough time for some diffusional exchange with the host matrix (Fig. 2). In contrast, the magnetites within these crystal clots appear to have completely rehomogenized to the composition of those in the rhyodacite host (Fig. 3). Diffusion is probably fast in iron oxides relative to pyroxenes, so that magnetites can re-equilibrate with their host before pyroxenes. Some rare plagioclase phenocrysts in the rhyodacite have cores up to $\sim An_{83}$ in composition (Carey 1982). These cores may be inherited grains from a mafic magma injected into the rhyodacite long ago. Taken together, the mafic inclusions indicate that there were multiple injections of mafic magma into the rhyodacite and these injections occurred over a protracted period of time.

Thermal evolution of the Minoan storage region

We have suggested that the Minoan rhyodacite was repeatedly invaded by mafic magma, which heated the rhyodacite from 825 ± 25 °C to 885 °C. Episodic replenishment of a magma by a hotter and more mafic magma has been modeled extensively (Huppert and Sparks 1980, 1984; Huppert et al. 1982; Sparks and Huppert 1984; Sparks and Marshall 1986). Here, we present a simple heat flow model to investigate the conditions and feasibility of raising the temperature of the rhyodacite magma body by as much as 85 °C, the maximum heating believed to have occurred. We begin with the assumption that the mafic input magma was basaltic, added incrementally, and that it lost heat convectively to the rhyodacite while it cooled and crystallized. At the same time, the rhyodacite lost heat to its surroundings. For a given mass of rhyodacite, and a known temperature change, the time needed for heating can be estimated from:

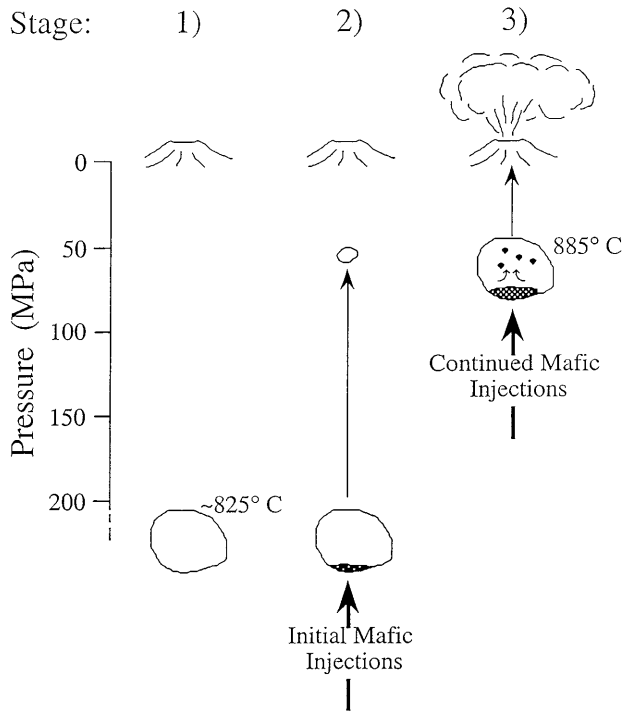

Fig. 9 Schematic cartoon illustrating the stages in the history of the Minoan magmas (neither volcano nor magma bodies are to scale). *Stage 1* At sometime in the past, the Minoan rhyodacite is stored at about 825 °C and pressures above 200 Mpa. *Stage 2* Mafic magma begins to be injected into the reservoir which forces the rhyodacite to a shallower level. *Stage 3* At least 30 km^3 of magma is temporarily stored in a reservoir at 50 MPa, where the magma is heated by continued injections of mafic magma, and then erupts cataclysmically. Parts of the mafic magma are entrained in the rhyodacite and are preserved as inclusions and scoria clasts. The amount of time spent in the shallow storage is at least 300 years, based on heat flow calculations (see text)

$$t = \frac{\left(\frac{M_D}{S}\right) C_P \Delta T_D}{Q_B - Q_{loss}} \quad (1)$$

where t is the time span for heating, M_D is the mass of rhyodacite, C_P is heat capacity, ΔT_D is the temperature change that the rhyodacite undergoes, S is area over which heat is exchanged, and Q_B and Q_{loss} are heat fluxes into and out of the rhyodacite. We set S equal to the area of the Minoan caldera (Druitt and Francaviglia 1992), assuming that it approximates the lateral dimensions of the rhyodacite storage zone.

Large uncertainties come into play when estimating Q_B and Q_{loss} because they depend highly on heat transfer mechanisms and physical parameters, such as viscosity and chamber geometry, that can vary immensely. Here, we are simply concerned with the range in relative magnitudes of Q_B and Q_{loss}. We can estimate Q_B from:

$$Q_B = \frac{\left(\frac{dM_B}{dt}\right) C_P (\Delta T_W)}{S} \quad (2)$$

where dM_B/dt is the mass flux of mafic magma. Crisp (1984) proposed an average value of $\sim 2 \times 10^{-2}$ km^3 yr^{-1} over the lifetime of large silicic volcanoes in subduction zones. ΔT_W is the difference in temperature between the incoming basalt and the convecting basaltic layer, which for our purposes is roughly 150 °C (Jaupart, pers. comm. 1998). Using those values and setting C_P = 2000 J kg^{-1} K^{-1} (which includes latent heat as a result of crystallization of the mafic magma; C. Jaupart, pers. comm. 1998), we estimate a heat flux of approximately 43 W m^{-2}.

Heat loss from the rhyodacite to the country rocks (Q_{loss}) can be estimated by:

$$Q_{loss} = \left[\frac{\lambda^2 \alpha (\Delta T_{EFF})^4 C_P g \rho_D^2}{R_C \eta_D} \right]^{1/3} \quad (3)$$

where λ is thermal conductivity, α is the coefficient of thermal expansion, g is gravitational acceleration, ρ_D is density of the rhyodacite, C_P is heat capacity, R_C is the critical Rayleigh number, and η_D is the viscosity of the rhyodacite. ΔT_{EFF} can be modeled using the variable viscosity model of Davaille and Jaupart (1993) whereby a stagnant region forms at the cooling boundary layer. ΔT_{EFF} is the difference in temperature between the convecting rhyodacite and the magma in the boundary layer that is able to convect. It is dependent on magma rheology and is generally on the order of 20 °C to 100 °C and does not vary significantly outside this range. Here we set ΔT_{EFF} to 30 °C as a result of the relatively high viscosity (Davaille and Jaupart, 1993). Using reasonable values for λ (1 W m^{-1} K^{-1}, Shimada et al. 1985; Snyder et al. 1994), α (5×10^{-5} K^{-1}; Lange and Carmichael 1990); C_P (1000 J kg^{-1} K^{-1}; Richet 1987), η_D (10^5 Pa s; Shaw 1972), ρ_D (2400 kg m^{-3}; Lange and Carmichael 1990), and R_C (10^3), we estimate Q_{loss} at approximately 30 W m^{-2}. When we combine this estimate with that for heat gained (Q_B = 43 W m^{-2}), we can solve for heating time using Eq. 1. This calculation suggests that roughly 300 years are needed to heat the rhyodacite from 800 °C to 885 °C. This estimate seems reasonable considering that our petrological observations indicate that there has been a long period of interaction between rhyodacite and mafic magma.

The above thermal modeling assumed that the volume of rhyodacite was constant. It is unknown how much volume actually existed in the deeper reservoir, although glass inclusions with >3.5 wt% water are common in both plagioclase and pyroxene phenocrysts. This implies that most of phenocrysts existed at depth, which may suggest that much of the total volume existed as well. On the other hand, there is compositional and petrologic evidence that assimilation of country rock was occurring at shallow depths (Druitt et al. in press), suggesting that volume was not constant. Detailed examination of phenocryst compositional zoning may help resolve this problem; however, uncertainty as to whether total volume was conserved does not alter our conclusions.

Pressure evolution of the Minoan storage region

Based on the experimental results and petrology of the erupted purmice, we suggest that the Minoan rhyodacite underwent large changes in pressure prior to erupting (Fig. 9). So far, water pressures have been assumed to equal total pressures. This was probably not strictly true when the melt inclusions were trapped, because they contain other volatile species (Cl, S, and F). Regardless, because water pressure was above 200 MPa when the inclusions formed, a rise to a 50-MPa storage region would create water saturation early in the ascent if it did not already exist, and saturation would be maintained thereafter. On the other hand, it could be argued that while water pressure was lowered to 50 MPa, total pressure remained above 200 MPa. This implies that the rhyodacite became about 75% undersaturated with water in the deep storage zone and, hence, degassed 3.0 to 3.5 wt% water, or about 2×10^{12} to 3.5×10^{12} kg from the ≥ 30 km^3 of magma (volume erupted). For this to occur, another volatile, such as CO_2 released from the mafic magma, must be added to decrease the activity of water; in this case, 1×10^{13} to 2.6×10^{13} kg of CO_2, must be added. If we assume that the mafic magma contained 0.2 to 0.3 wt% CO_2, the amount estimated for primary basaltic melts (as summarized by Johnson et al. 1994), then a minimum of 1600 to 2900 km^3 of mafic magma is required to degas in order to lower water pressure to 50 MPa in the rhyodacite. These volumes are minima because the calculations assume that no water degasses from the mafic magma. This dilution of P_{H_2O} with CO_2 seems unlikely, not only because it requires such a massive volume of basaltic magma, but also because the heat loss from such a large volume of crystallizing basalt (it would have to crystallize to degas) would undoubtedly have heated the rhyodacite much more than 85 °C. We conclude that our estimated change in pressure is a change in total pressure, and thus a rise in the crust of roughly 5 to 6 km.

Studies of the Kameni Islands, a volcanic dome complex erupted inside the Minoan caldera in the last ~2,000 years, support the idea of a shallow magmatic zone beneath Santorini (Barton and Huijsmans 1986). The Kameni domes are dacites (64 to 68 wt% SiO_2), that contain 15 to 20 vol.% phenocrysts, mainly of plagioclase, clinopyroxene, and orthopyroxene; no hornblende has been reported. Temperatures estimated for these magmas range from 960 to 1012 °C (Barton and Huijsmans 1986). In order for such relatively hot dacites to be 15 to 20 vol.% crystallized, water pressures must have been very low, according to phase equilibria determined for compositionally similar dacites from Mount St. Helens and Mount Rainier (Rutherford et al. 1985; Venezky and Rutherford 1997). This suggests that the Kameni Island dacites were stored in the same shallow region established by the Minoan rhyodacite.

Geophysical evidence indicates that the present-day contact between basement (density of 2600 kg m^{-3}) and sedimentary caldera fill (density of 2300 kg m^{-3}) lies at approximately 1.6 km beneath Santorini (Druitt et al. in press). This boundary undoubtedly marks caldera fill from the Minoan eruption, but it is probably also partially related to the collapse of several pre-Minoan calderas (Druitt and Francaviglia 1992). This marks a pressure of about 36 MPa, similar to where the Minoan rhyodacite was last equilibrated. Such a lower density sedimentary layer may have acted to slow the ascent of the Minoan rhyodacite from its deep reservoir, causing it to pond a shallow level without erupting.

The model presented here suggests that a large body of magma moved relatively quickly within the crust by 5 to 6 km. Similarly, Gardner et al. (1995) presented evidence that the depth of the magma storage region beneath Mount St. Helens has moved twice by 3 to 5 km, both times in less than 100 years. How common are these upward movements of magma storage zones in the crust? Interestingly, the cataclysmic eruption of Mount Mazama (Crater Lake) was very similar to the Minoan eruption, with a large volume of homogeneous rhyodacite magma containing mafic scoria being erupted (Bacon 1983; Druitt and Bacon 1989). In both cases, the temperature of the rhyodacite was about 880 °C and there is convincing evidence for essentially syn-eruptive injection of at least some of the mafic scoria. However, the Mazama rhyodacite contains phenocrystic amphibole, placing its storage zone at a somewhat greater depth than that of the Minoan (Fig. 4) and there is presently no evidence for a pre-eruption pressure change in the Mazama products. This indicates that although magmatic movements beneath volcanoes can occur, they are not ubiquitous. It is possible that the prior history of multiple caldera-forming eruptions at Santorini facilitated magma ascent.

Conclusions

Most magma exhumed during the caldera-forming Minoan eruption of Santorini volcano, Greece, was homogeneous rhyodacite, while a small volume of mafic magma was also erupted (Druitt et al. 1989). Through a combination of petrologic and experimental observations on samples of the rhyodacite, andesite, and their intermingled hybrids, we have derived a three stage model for the evolution of the magma storage region leading up to the eruption (Fig. 9):

(1) Magma was stored at relatively high water pressures of 210 to 240 MPa and at a temperature of 825 ± 25 °C. The rhyodacite at this stage consisted of water-rich rhyolitic melt and phenocrysts of plagioclase ($An_{56 \pm 6}$), pyroxene, FeTi oxides, and amphibole.

(2) Injection of mafic magma forced the rhyodacitic magma out of the deep reservoir toward shallower pressures. Most of the interaction between rhyodacite and mafic magma probably occurred at shallow levels, as required to preserve plagioclase phenocrysts with glass inclusions trapped at high pressures (plagioclase is unstable at temperatures above ~850 °C at 200 MPa).

(3) Rhyodacitic magma ponded in the crust where it was stored at a pressure of about 50 MPa and a temperature of 885 °C. A crustal density change may have caused the rhyodacite to stall in the crust at shallow levels, but uncertainties about crustal density structure prior to the collapse of the Minoan caldera make this speculative. Simple heat flow modeling suggests that, assuming a reasonable input rate of mafic magma and heat loss to country rock, that at least 300 years are required to heat the rhyodacite to 885 °C. This is in agreement with our observations of homogeneous ~100-μm diameter magnetite and ilmenite phenocrysts in the rhyodacite and partial re-equilibration of mafic magma inclusions in the rhyodacite. Mafic scoria containing stable groundmass hornblende represent injections of mafic magma into the shallow reservoir within several days of the Minoan eruption; the lath-shaped hornblende crystals could not have survived breakdown for longer times at this depth. Dacites erupted since the Minoan eruption (forming the Kameni Islands) appear to have been tapped from the shallow level magma storage zone established by the Minoan rhyodacite.

Acknowledgements The authors wish to thank Tim Druitt for his kind donation of andesite samples and helpful discussions on the scoria clasts. Sample S-814 was kindly supplied by the Marine Geological Samples Laboratory supported by NSF grant OCE-9402059 for curatorial services at the Graduate School of Oceanography, University of Rhode Island. We are in debt to Claude Jaupart for his extensive help with the thermal modeling. Discussions with Don Synder, Steve Tait, and Marc Parmentier are also greatly appreciated. We thank Joseph Devine for assistance with electron microprobe analyses and Etienne Deloule for assistance with the secondary ion mass spectrometry analyses. Fieldwork by JEG on Santorini and SIMS analyses could not have occurred without the generosity of Claude Jaupart. Thoughtful reviews by Steve Sparks and Charlie Bacon improved the manuscript greatly. This study was partially funded by NSF grant EAR-9526527 and a Royce Fellowship from Brown University (to EC).

References

Andersen DJ, Lindsley DH (1988) Internally consistent solution models for Fe-Mg-Mn-Ti oxides: Fe-Ti oxides. Am Mineral 73: 714–726

Andersen DJ, Lindsley DH, Davidson PM (1993) QUILF: a Pascal program to assess equilibria among Fe-Mg-Ti oxides, pyroxenes, olivine and quartz. Computers and Geosciences, v. 19, 1333–1350.

Bacon CR (1983) Eruptive history of Mount Mazama and Crater Lake caldera, Cascade Range, USA. J Volcanol Geotherm Res 18: 57–115

Bacon CR, Hirschmann MM (1988) Mg/Mn partitioning as a test for equilibrium between coexisting Fe-Ti oxides. Am Mineral 73: 57–61

Barton M, Huijsmans JPP (1986) Post-caldera dacites from the Santorini volcanic complex, Aegean Sea Greece: an example of the eruption of lavas of near-constant composition over a 2,200 year period. Contrib Mineral Petrol 94: 472–495

Blank JG, Stolper EM, Carroll MR (1993) Solubilities of carbon dioxide and water in rhyolitic melt at 850 °C and 750 bars. Earth Planet Sci Lett 119: 27–36

Bond A, Sparks RSJ (1976) The Minoan eruption of Santorini, Greece. J Geol Soc London 312: 1–16

Carey SN (1982) Studies of tephra dispersal and deposition. Unpub. PhD Thesis, University of Rhode Island, Kigston, RI

Carroll MR, Rutherford MJ (1985) Sulfide and sulfate saturation in hydrous silicate melts. J Geophys Res 90: 601–612

Crisp JA (1984) Rates of magma emplacement and volcanic output. J Volcanol Geotherm Res 20: 177–211

Davaille A, Jaupart C (1993) Thermal convection in lava lakes. Geophys Res Let 20: 1827–1830

Devine JD, Gardner JE, Brack HP, Layne GD, Rutherford MJ (1995) Comparison of microanalytical methods for estimating H_2O contents of silicic volcanic glasses. Am Mineral 80: 319–328

Druitt TH, Bacon CR (1989) Petrology of the zoned calcakaline magma chamber of Mount Mazama, Crater Lake, Oregon. Contrib Mineral Petrol 101: 245–259

Druitt TH, Francaviglia V (1992) Caldera formation on Santorini and the physiography of the islands in the late Bronze Age. Bull Volcanol 54: 484–493

Druitt TH, Mellors RA, Pyle DM, Sparks RSJ (1989) Explosive volcanism on Santorini, Greece. Geol Mag 126: 95–126

Druitt TH, Edwards L, Mellors RM, Pyle DM, Sparks RSJ, Lauplare M, Davies M, Barreirio B (in press) Santorini Volcano. Mem Geol Soc London

Fogel R (1989) The role of C-O-H-Si volatiles in planetary igneous and metamorphic processes: experimental and theoretical studies. PhD Thesis, Brown University, Providence

Gardner JE, Rutherford M, Carey S, Sigurdsson H (1995) Experimental constraints on pre-eruptive water contents and changing magma storage prior to explosive eruptions of Mount St Helens volcano. Bull Volcanol 57: 1–17

Gardner JE, Thomas RME, Jaupart C, Tait S (1996) Fragmentation of magma during Plinian volcanic eruptions. Bull Volcanol 58: 144–162

Geschwind C-H, Rutherford MJ (1992) Cummingtonite and the evolution of the Mount St. Helens magma system: an experimental study. Geology 20: 1011–1014

Heiken G, McCoy F (1984) Caldera development during the Minoan eruption, Thira, Cyclades, Greece. J Geophys Res 89: 8441–8462

Huppert HE, Sparks RSJ (1980) The fluid dynamics of a basaltic magma chamber replenished by influx of hot, dense ultrabasic magma. Contrib Mineral Petrol 75: 279–289

Huppert HE, Sparks RSJ (1984) Double-diffusive convection due to crystallization in magmas. Ann Rev Earth Planet Sci 12: 11–37

Huppert HE, Turner JS, Sparks RSJ (1982) Replenished magma chambers: effects of compositional zonation and input rates. Earth Planet Sci Lett 57: 345–357

Johnson MC, Anderson AT, Jr, Rutherford MJ (1994) Pre-eruptive volatile contents of magmas. In: Carroll MR, Holloway JR (eds) Volatiles in magmas (Reviews in Mineralogy vol. 30). Mineralogical Society of America, Washington DC, pp 447–478

Lange RA, Carmichael I (1990) Thermodynamic properties of silicate liquids with emphasis on density, thermal expansion and compressibility. In: Nicholls J, Russell JK (eds) Modern methods of igneous petrology (Reviews in Mineralogy vol. 24). Mineralogical Society of America, Washington DC, pp 25–64

Nakamura M (1995) Continuous mixing of crystal mush and replenished magma in the ongoing Unzen eruption. Geology 23: 807–810

Richet P (1987) Heat capacity of silicate glasses. Chem Geol 62: 111–124

Rutherford MJ, Devine JD (1996) Preeruption pressure-temperature conditions and volatiles in the 1991 dacitic magma of Mount Pinatubo. In: Newhall CG, Punongbayan RS (eds) Fire and mud: eruptions and lahars of Mount Pinatubo, Philippines. University of Washington Press, Seattle, pp 751–766

Rutherford MJ, Sigurdsson H, Carey S, Davis A (1985) The May 18, 1980, eruption of Mount St. Helens, 1, Melt composition and experimental phase equilibria. J Geophys Res 90: 2929–2947

Shaw HR (1972) Viscosities of magmatic liquids: an empirical method of prediction. Am J Sci 272: 870–893

Shimada M, Scarfe CM, Schloessin HH (1985) Thermal conductivity of sodium disilicate melt at high pressures. Phys Earth Planet Inter 37: 206–213

Sigurdsson H, Carey S, Devine JD (1990) Assessment of mass, dynamics, and environmental effects of the Minoan eruption of Santorini Volcano. In: Hardy D (ed) Thera and the Aegean world III, Vol 2. Thera Foundation, London, pp 100–112

Silver LA, Ihinger PD, Stolper EM (1990) The influence of bulk composition on the speciation of water in silicate glasses. Contrib Mineral Petrol 104: 142–162

Synder D, Gier E, Carmichael I (1994) Experimental determination of the thermal conductivity of molten $CaMgSi_2O_6$ and the transport of heat through magmas. J Geophys Res 99: 15503–15516

Sparks RSJ, Huppert HE (1984) Density changes during the fractional crystallization of basaltic magmas: implications for the evolution of layered intrusions. Contrib Mineral Petrol 85: 300–309

Sparks RSJ, Marshall L (1986) Thermal and mechanical constraints on mixing between mafic and silicic magmas. J Volcanol Geotherm Res 29: 99–124

Sparks, RSJ, Wilson CJN (1990) The Minoan deposits: a review of their characteristics and interpretation. In: Hardy D (ed) Thera and the Aegean world III, Vol 2. Thera Foundation, London, pp 89–99

Stormer JC (1983) The effects of recalculation on estimates of temperature and oxygen fugacity from analyses of multi-component iron-titanium oxides. Am Mineral 68: 586–594

Venezky DY, Rutherford MJ (1997) Preeruption conditions and timing of dacite-andesite magma mixing in the 2.2 ka eruption at Mount Rainier. J Geophy Res 102: 20069–20086

Venezky DY, Rutherford MJ (in press) Petrology and FeTi oxide reequilibration of the 1991 Mount Unzen mixed magma. J Volcanol Geotherm Res